Springer

KSME

Journal of Mechanical Science and Technology 24 (8) (2010) 1603~1609
www.springerlink.com/content/1738-494x
DOI 10.1007/s12206-010-0512-3

# Single-point diamond turning of electroless nickel for flat X-ray mirror †

Kwon Su Chon[1,*] and Yoshiharu Namba[2]

[1]*Department of Radiological Science, Catholic University of Daegu, Gyeongbuk 712-702, Korea*
[2]*Department of Mechanical Egineering, Chubu University Aichi 487-8501, Japan*

(Manuscript Received May 4, 2009; Revised April 20, 2010; Accepted May 1, 2010)

**Abstract**

X-ray mirrors require a super-smooth surface to prevent strong X-ray scattering. We examined the fabrication possibility of the X-ray mirror by single-point diamond turning (SPDT) for electroless nickel. The stable and unstable cutting modes for the electroless nickel were obtained by observing the relative position of a diamond tool for machining. A super-smooth surface of 0.95 nm rms was achieved within the stable cutting mode. The surface roughness of the electroless nickel mirror measured with an optical profiler was compared with the X-ray reflectivity measurement. The electroless nickel mirror could be successfully used as a soft X-ray reflector and a low-pass filter for the hard X-rays.

*Keywords*: Electroless nickel; Single-point diamond turning; Surface roughness; Ultraprecision machining; X-ray mirror

## 1. Introduction

Metal cutting using an ultraprecision machine tool and a diamond tool had begun in 1960's and through 1970's, the machine tool had considerable been improved by advancing of the numerical control system and the accurate position metrology using a laser interferometer [1]. Single-point diamond turning (SPDT) is an excellent optical finishing technique and is easy to generate aspheric shape compared to traditional methods. Owing to these merits, the SPDT has various applications, mainly optical elements.

Generally, non-ferrous metals and plastics can be used in the SPDT [2]. The well-known metal materials are aluminum alloys, oxygen-free copper, and electroless nickel that is an alloy of nickel and phosphorus. From a material point of view, the surface topography after the SPDT depends on some material aspects such as purity, grain size, and anisotropy [3, 4]. Thus, the selection of a material is very important to obtain a super-smooth surface. In this sense, electroless nickel of an amorphous structure is one of excellent materials in the SPDT. In addition, electroless nickel has been widely used in industrial and optical applications [5-6].

The properties of the electroless nickel largely depend on the percentage of phosphorus and the heat treatment temperature. It is generally agreed that the nickel-phosphorus alloys containing less than 7% phosphorus are microcrystalline and those in the 7 to 14% phosphorous range show amorphous [7]. Talyer et al. [8] investigated surface roughness by the SPDT for electroless nickel samples having combinations of various phosphorus contents and heat treatment temperatures.

X-ray mirrors using total reflection require a super-smooth surface because the X-ray wavelength is very short, nanometer or sub-nanometer scales; otherwise the X-rays suffer from strong scattering on the reflecting surface. In addition, X-ray reflection largely depends on the material property, that is, the electron density of the mirror material. From the optical point of view, electroless nickel is one of the best materials as the mirror material for soft X-rays of a few nanometers wavelength.

In this paper, we deal with the SPDT of electroless nickel containing about 10 weight percent phosphorus plated on flat aluminum alloy, A7075, samples. The relation between surface roughness and cutting conditions is examined to obtain super-smooth surface by the SPDT. We also discuss the X-ray reflectivity for a diamond-turned electroless nickel flat mirror.

## 2. Single-point diamond turning

Generally, electroless nickel is plated on aluminum alloys or steel. We prepared electroless nickel plated on the aluminum alloy, A7075. The thickness and the diameter of aluminum alloy substrate were 12 mm and 58 mm, respectively. Nickel plating was done for ten hours, and the thickness of the electroless nickel was approximately 110 μm, which contained about 10 percent phosphorus. The electroless nickel had

† This paper was recommended for publication in revised form by Associate Editor Dae-Eun Kim

*Corresponding author. Tel.: +82 53 850 3437, Fax.: +82 53 850 3292
E-mail address: kschon@cu.ac.kr

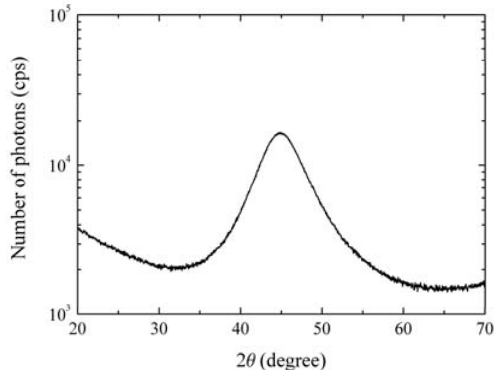


Fig. 1. X-ray diffraction measurement for an electroless nickel sample which shows the amorphous structure.

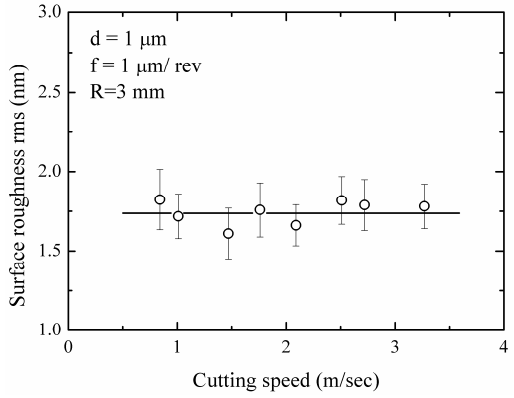


Fig. 2. Relation between surface roughness and cutting speed under 1 μm in depth of cut (d), 1 μm/rev in feed rate (f), and 3 mm in nose radius (R).

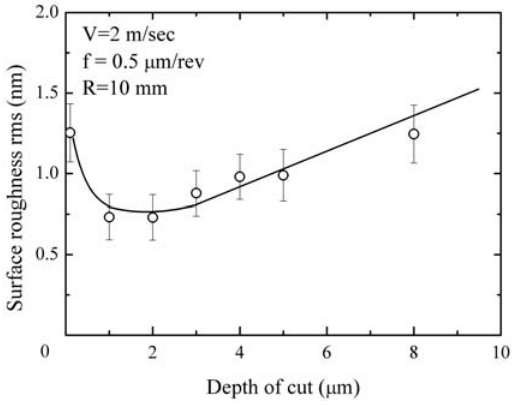


Fig. 3. Relation between surface roughness and depth of cut under 2 m/sec in cutting speed (V), 0.5 μm/rev in feed rate (f), and 10 mm in nose radius (R).

amorphous structure. Fig. 1 shows an x-ray diffraction pattern for an electroless nickel sample. The maximum peak appeared at $2\theta = 44.5°$ of which angle position corresponded to the peak position of diffraction by (111) plane of pure nickel.

The diamond turning machine tool (AHN-10, TOYOTA) used in this experiment has two perpendicular slide tables (Z and X axes), an air bearing spindle on the Z-slide table, and a rotary table (B-axis) with a tool post. A laser interferometer system was used to determine positions accurately. X and Z-tables could be controlled within 1 nm positional step. The B-table could be rotated with an angular step of 0.0001°. However, in this experiment the B-table was fixed for the face machining. The machine tool was set up within a vibration isolator and supported by air mounts to prevent external vibrations. The environment was maintained in a clean room of class 100 and controlled within a temperature of 0.1 K. A sample was loaded on the vacuum chuck, and the kerosene mist with air pressure of 0.2 MPa was sprayed on the sample, which also assisted in removing chips during machining.

Single-crystal diamond tools for which the crystallographic plane (110) was rake face were used, and rake and clearance angles were 0 and 5 degrees, respectively. The window angle was 90 degrees. The shank of diamond tools was made of steel.

The samples used in investing surface roughness behaviors in terms of cutting conditions were divided into five sections with different boundary radii, and the machined surface was examined with a Nomarski microscope and measured with an optical profiler (ZYGO New View 200 HR with 20 X magnification objective). The measured area was 360 μm × 270 μm.

## 3. Surface roughness and cutting conditions

Surface roughness was really independent of cutting speed of from 0.5 m/sec to 3.6 m/sec. Fig. 2 shows the relation between surface roughness of rms (root-mean-square) value and cutting speed. Error bar stands for the standard deviation for each measurement. The average surface roughness and the average standard deviation were 1.75 nm rms and 0.32 nm, respectively. The surface roughness under different cutting conditions, i.e., different nose radii (5 mm and 10 mm), depth of cut (2 μm and 3 μm), and feed rates (0.8 μm/rev and 1.5 μm/rev), also showed constant behaviors. It meant that the cutting force was almost constant, which was indirectly inferred from the chip behavior. There was no chip rubbing.

Surface roughness with respect to the depth of cut showed almost constant behavior between 1 μm and 3 μm within standard deviation as shown in Fig. 3, and the machined surface showed the best quality. However, as increasing the depth of cut (from 3 μm roughly), the surface roughness had a tendency to increase at a very low rate. The surface roughness increased when the depth of cut was from 1 μm (actually, between 0.5 μm and 1 μm) to the lowest depth of cut, which gave a whole cut on the sample without partial cut. In this range, the machined surface strongly was affected by the spindle motion errors. The yawing error of the air spindle was approximately 0.1 μm, which was measured with an accelerometer to check the spindle motion. The yawing error corresponded to the angle deviation of $3.3\times10^{-6}$ rad with respect to the rotation center. Thus, the surface roughness might increase because the displacement deviation of the depth direction

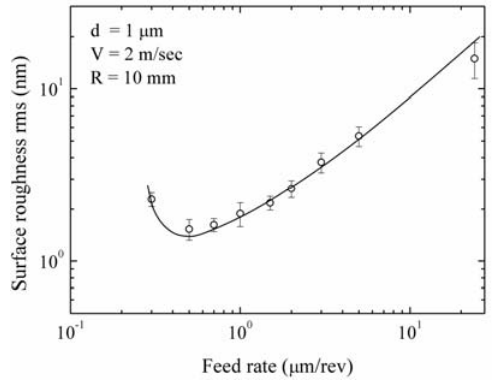


Fig. 4. Relation between rms surface roughness and feed rate for a nose radius of 10 mm.

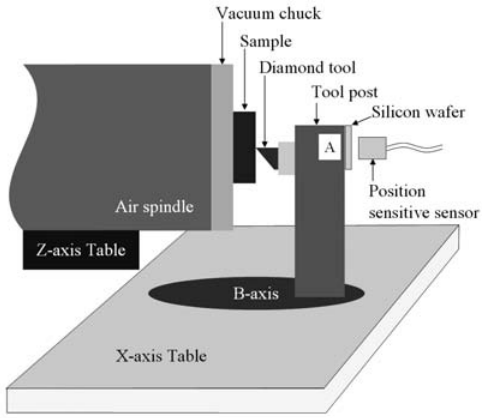


Fig. 5. Schematic configuration of the relative tool position measurement.

might be maximally 0.19 μm, which came from the spindle angle deviation times the sample diameter of 52 mm. Therefore, the spindle motion error could have a the strong influence on the surface roughness in very low depth of cut, less than 0.5 μm. Additionally, a tiny chip mixed with mist oil was attached on the diamond tool and the chip removal was not easy, which resulted in the surface degradation. There is a critical depth of cut for transition from ductile mode to brittle mode for brittle materials [9]. Electroless nickel is a brittle material. The critical depth of cut is above 10 μm for the electroless nickel [10].

A depth of cut of more than 0.5 μm and cutting speed from 0.5 m/sec to 3.6 m/sec were not critical factors to influence to the surface quality of electroless nickel samples under the fixed feed rate. The tool marks on the surface of the electroless nickel strongly depended on the feed rate as well as the residual stress, friction, and subsurface plastic flow. The surface roughness of an ultraprecision machined sample is largely influenced by the machine kinematics at high feed rate, but significantly influenced by other factors at a lower feed rate [11]. Fig. 4 shows the relation between surface roughness in the rms value and feed rate for a nose radius of 10 mm. Open circles and solid line present experimental data and fitted curve, respectively. The experimental data shown in Fig. 4 were obtained from samples machined with a cutting speed of 2 m/sec and a depth of 1 μm. The surface roughness showed similar behavior compared to the theoretical estimation even if the values were different. It could result from the inherent machine tool vibration which made a dominant waviness of 120 μm in spatial wavelength on the machined surface. However, at very low feed rate of less than 0.5 μm/rev the surface roughness was increased. In this range, the surface roughness largely depended not on the feed rate and the nose radius of the diamond tool but other factors such as high-frequency vibration and chip removal.

There was a low limit in the depth of cut and the feed rate to achieve a high quality surface. To examine the relation between cutting conditions and the working condition of the machine tool, we observed the relative position of the diamond tool by a gap sensor for machining of the electroless nickel. Fig. 5 shows the schematic configuration of the relative tool position measurement. A gap sensor was strongly fixed on the X-axis table, and the relative position of the diamond tool in the vertical direction to the machined surface was monitored with a position sensitive sensor which gener-

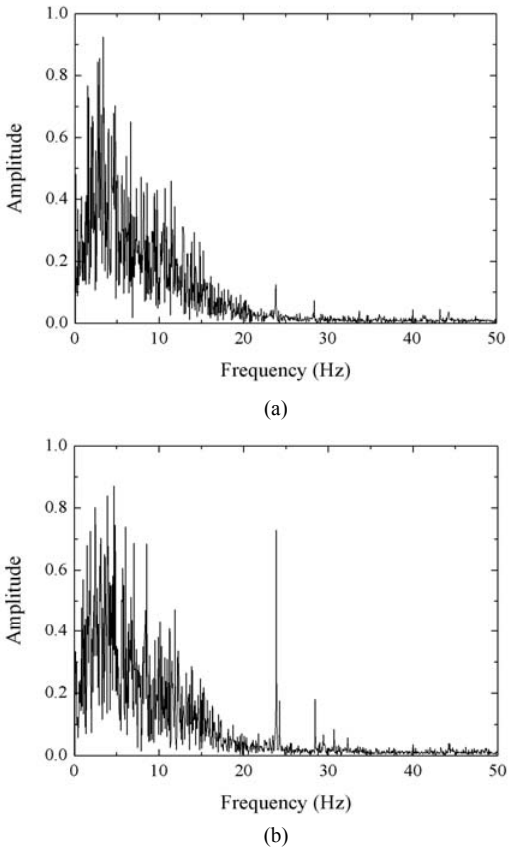


Fig. 6. Frequency response for stable (a) and unstable (b) cutting modes in observing the relative position displacement of diamond tool during machining of electroless nickel.

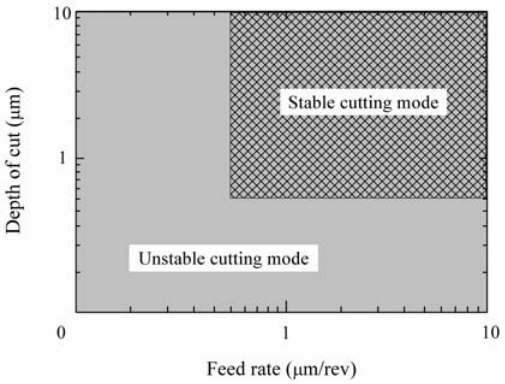


Fig. 7. Stable and unstable cutting modes of single-point diamond turning for electroless nickel.

ated "voltage" according to the distance between the sensor and a piece of silicon wafer. The silicon wafer was attached on the tool post and was parallel to the machined surface of the electroless nickel. The smooth surface of the silicon wafer reduced the noise level within the signal. The voltage signal through the A/D converter was analyzed by fast Fourier transform. The sampling time for the voltage signal was 10 msec. We found that the frequency of 23.8 Hz was enhanced in the unstable cutting mode as shown in Fig. 6(b). The enhancement of the 23.8 Hz critically depended on very low feed rate and very small depth of cut. Fig. 7 shows stable and unstable cutting modes of the SPDT for electroless nickel samples with respect to the depth of cut and the feed rate. A smooth surface could be obtained within the stable cutting mode, and the boundary between two modes might depend on detail cutting environments such as machine tool condition, nose radius and wear of the tool, and chip removal. The stable cutting mode means that the surface roughness of electroless nickel is lower as decreasing the feed rate and the depth of cut. However, the surface roughness is larger as decreasing the feed rate and the depth of cut in the unstable cutting mode. Fig. 8 shows Nomarski microscope images for the stable and unstable cutting modes in the SPDT of the electroless nickel.

The mode was derived from the measurement of the vibration frequency, and the mode was very similar to the combination of the relations between the surface roughness and the depth of cut and the surface roughness and the feed rate. If either of the depth of cut or the feed rate was very low, the cutting mode became unstable. The resonance of the machine tool [12] was closely related to the low depth of cut and the feed rate. The resonance might be connected to the B-axis. The B-table was fixed on the X-table, but the servo system of the B-axis was working. Because the rigid tool post was positioned on the B-table, the origin of the vibration could be B-table. The relative angle variation of the B-table was $\pm 0.0002°$, which was verified by checking the numerical controller with respect to the B-axis and by measuring the position deviation at the position of the marked "A" on the tool post as shown in Fig. 5. The angle variation by the later

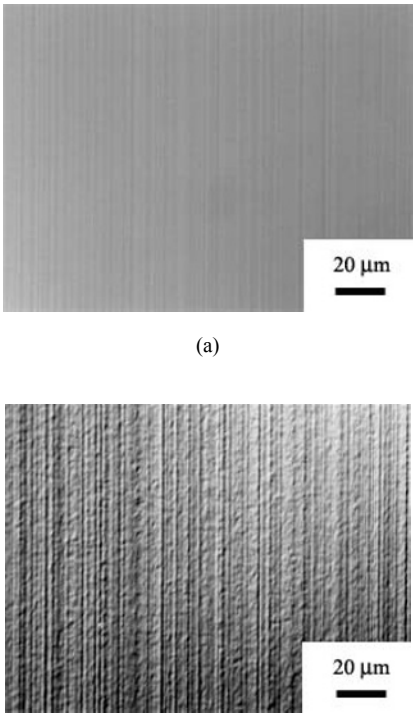


Fig. 8. Nomarski microscope surface images for stable (a) and unstable (b) cutting modes of single-point diamond turning for flat electroless nickel.

measurement was very close to the former. Although the effect by the angle variation at the center of B-axis, i.e., the cutting edge of the diamond tool, was very small, the angle variation of the B-axis would be one of the vibration sources.

The machined surface depends on wear of the single-crystal diamond tool. In our experiment, after 33 km in cutting distance the minor tool wears were detected on the rake and the flank faces which were observed with the Nomarski microscope. Up to the distance, there was no degradation of the electroless nickel surface. We found surface deterioration after 50 km in cutting distance. Other studies for the electroless nickel also show no surface change before 40 km [13] and 50 km [14]. To remove the tool wear effect on the surface roughness, we changed the cutting edge of the single-crystal diamond tool by rotation of 0.5 degree after around every 20 km in cutting distance.

## 4. Reflectivity study

The electroless nickel shows good optical properties, especially reflectivity in the soft X-ray region. It is one of the excellent optical substrates used in soft x-ray optics and synchrotron optics [15]. We made a flat electroless nickel mirror under cutting conditions of 10 mm in nose radius, 1 μm in depth of cut, and 0.5 μm/rev in feed rate. The surface roughness of the electroless nickel mirror was 0.95 nm rms with a standard deviation of 0.25 nm in 360 μm × 270 μm area. The surface

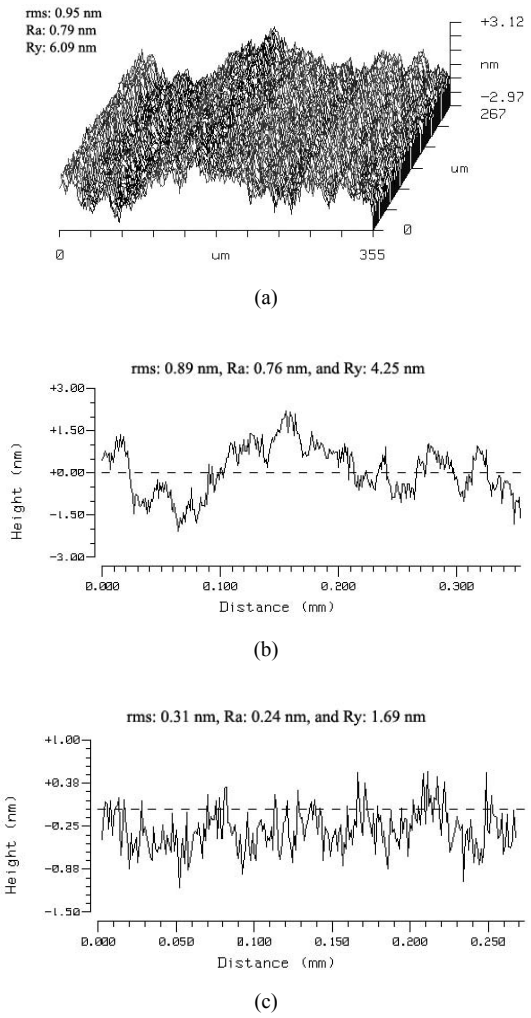


Fig. 9. Surface profiles for an electroless nickel mirror (b) and (c) show the vertical and parallel direction profiles for (a).

roughness value was approximately ten times better than other studies [10, 14] for the electroless nickel. Fig. 9(a) shows the measured surface for the machined electroless nickel surface, and Fig. 9(b) and (c) are profiles for vertical and parallel directions to the tool marks. The surface roughnesses for the vertical and parallel directions were, respectively, 0.89 nm and 0.31 nm, and the surface roughness for the parallel direction was very small compared to those for the area and the vertical direction.

The surface roughness as the rms value could be estimated from the X-ray reflectivity measurement. Fig. 10 shows X-ray reflectivities at the $Cu_{K\alpha}$ emission line ($\lambda$= 0.154 nm in wavelength) for the parallel and vertical directions, which means that the incident X-rays are parallel and vertical to the tool marks on the electroless nickel surface. During an angle scan of the sample using the X-ray, the scan height and minimum width were 0.1 mm and 4.5 mm, respectively. From the best fitting-curves for each measured reflectivity, the surface roughnesses for the parallel and vertical directions were 1.09

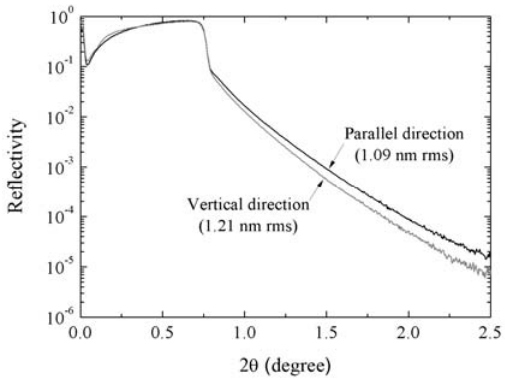


Fig. 10. X-ray reflectivity for parallel and vertical directions to cutting tool marks.

nm rms and 1.21 nm rms, respectively. These values were very close to the measurement value of the optical profiler, 0.95 nm rms. Although the two roughness values were slightly different (10 % difference), the values for both directions were not quite different like the line profiles shown in Fig. 9(b) and (c). The difference of two vertical directional surface roughnesses measured with the optical profiler and the X-ray reflectometer was 0.32 nm, which might result from the effects of low spatial frequencies, i.e., figure error, on the surface. From both different measurements, we can see that the rms surface roughness ($\sigma$) is presented by

$$\sigma = \sqrt{\sigma_{VD}^2 + \sigma_{PD}^2} \tag{1}$$

when one-dimensional surface profiles, for example, Fig. 9(b) and (c), are used to measure roughness for a surface of no isotropy property like the diamond-turned electroless nickel. $\sigma_{VD}$ and $\sigma_{PD}$ are rms surface roughnesses for the vertical and parallel directions, respectively.

X-ray reflectivity ($R$) on the machined electroless nickel mirror can be written as [16]

$$R = R_0 e^{-(4\pi\sigma\sin\theta/\lambda)^2} \tag{2}$$

where $R_0$ is the theoretical reflectivity [17] on the ideal interface and a function of the grazing incident angle of X-ray ($\theta$) and the optical constant [18] of the electroless nickel. $\lambda$ and $\sigma$ are the wavelength of X-ray and the rms surface roughness of the electroless nickel mirror. To obtain high reflectivity on the machined electroless nickel mirror, the surface roughness should be less than the wavelength of X-ray used [19], and the incident angle is generally less than the critical angle of X-ray. In practical applications, the incident angle is less than 2 degrees. For soft X-rays, especially the 'water window' (2.3 ~ 4.4 nm in wavelength) [20], the calculated reflectivity is over 0.8 at a surface roughness of 1.21 nm rms. It means that the electroless nickel surface machined by the SPDT can directly be used as a soft X-ray reflector without any post finish, for

example, polishing, and this fabrication method can be applied to manufacture aspheric X-ray mirrors. The diamond-turned electroless nickel mirror can also be used as an X-ray low-pass filter. Low energy X-rays easily can be removed by a thin solid filter. However, high energy X-rays have high transmission property. So, it is not easy to remove the high energy X-ray in broad band spectrum. Using the X-ray reflection on the electroless nickel mirror, low energy X-rays of less than 0.9 keV can be reflected with a high reflection efficiency of over 80%, but the high energy X-rays of over 3 keV are surely removed at an incident angle of 2 degrees.

## 5. Conclusions

The fabrication possibility of X-ray mirror by the SPDT was examined. Electroless nickel plated on flat aluminum alloy was used for the SPDT. The surface roughness of the electroless nickel was nearly independent of the cutting speed and the depth of cut of 1 μm to 3 μm. When depth of cut was, however, less than 0.5 μm, the surface roughness was increased. In the feed rate of less than 0.5 μm /rev the surface quality was degraded.

By observing the relative position of the diamond tool for machining, the stable and unstable cutting modes in terms of the feed rate and the depth of cut were obtained and were very close to the combination of the relations between the surface roughness and the depth of cut and the surface roughness and the feed rate. In the sable cutting mode, a surface roughness of 0.95 nm rms was achieved.

X-ray reflectivity measurement for an electroless nickel flat mirror showed no strong directional dependence for parallel and vertical directions, contrary to the line profiles measured with the optical profiler. There was no difference in the surface roughness values by X-ray reflectivity measurement and an optical profiler within a standard deviation. The electroless nickel machined by the SPDT without any post finish can successfully be used as a soft X-ray reflector and a low-pass filter for hard X-rays.

## Acknowledgment

This reasearch was supported by Basic Science Research Program through the National Research Foundation of Korea (NRF) funded by the Ministry of Education, Science and Technology (No. 20100005661) and supported in part by a Grant-in-Aid for Scientific Research (B) Nos. 15360075, 18360073 and 22360063 from the Japan Society for the Promotion of Science and a Grant-in-Aid for Exploratory Research (No. 16656054) from the Ministry of Education, Culture, Sports, Science and Technology, Japan.

## References

[1] C. J. Evans, Precision Engineering: An Evolutionary View, Cranfield Press, Cranfield, UK, (1989).

[2] R. L. Rhorer and C. J. Evans, Fabrication of optics by diamond turning, *OSA Handbook of Optics, 2nd Ed., Vol. 1*, McGraw-Hill, Washington DC, USA (1995).

[3] Z. Yean, W. Lee, Y. Yao and M. Zhou, Effect of crystallographic orientations on cutting force and surface quality in diamond cutting of single crystal, *Ann. CRIP* 43 (1) (1994) 39-42.

[4] M. Sato, T. Yamazaki, Y. Shimizu and T. Takabayashi, A study on the microcutting of aluminum single crystals, *JSME Int. J. Series C* 34 (4) (1991) 540-545.

[5] S. C. Fawcett and D. Engelhaupt, Development of Wolter I x-ray optics by diamond turning and electrochemical replication, *Prec. Eng*. 17 (4) (1995) 290-297.

[6] M. J. Boyle and H. G. Ahlstrom, Imaging characteristics of an axisymmetric grazing incidence x-ray microscope designed for laser fusion research, *Rev. Sci. Instrum*. 49 (6) (1978) 746-751.

[7] D. L. Hibbard, Electroless nickel for optical applications, *Proc. SPIE CR67* (1997) 179-205.

[8] J. S. Taylor, C. K. Syn, T. T. Saito and R. R. Donaldson, Surface finish measurements of diamond-turned electroless-nickel-plated mirrors, *Opt. Eng*. 25 (9) (1986) 1013-1020.

[9] T. Moriwaki, E. Shamoto and K. Inoue, Ultra-precision ductile cutting of glass by applying ultrasonic vibration, *Ann. CIRP* 41 (1992) 141-144.

[10] A. Pramanik, K. S. Neo, M. Rahman, X. P. Li, M. Sawa and Y. Maeda, Cutting performance of diamond tools during ultra-precision turning of electroless-nickel plated die materials, *J. Mater. Process. Technol*. 140 (2003) 308-313.

[11] N. P. Hung, Z. W. Zhong, K. K. Lee and C. F. Chai, Precision grinding and facing of copper-beryllium alloys, *Prec. Eng*. 23 (1999) 293-304.

[12] J. K. Myler, R. A. Parker and A. B. Harrison, High quality diamond turning, *Proc. SPIE* 1333 (1990) 58-62.

[13] C. J. Evans, R. S. Polvani and A. Mayer, Diamond turning electro-deposited nickel alloys, *OSA Technical Digest Series* 9 (1990) 110-113.

[14] K. M. Rezaur Rahman, M. Rahman, K. S. Neo, M. Sawa and Y. Maeda, Microgrooving on electroless nickel plated materials using a single crystal diamond tool, *Int. J. Adv. Manuf. Technol*. 27 (2006) 911-917.

[15] R. A. Paquin and M. R. Howells, Mirror materials for synchrotron radiation optics, *Proc. SPIE* 3152 (1997) 2-16.

[16] A. G. Michette, Optical system for soft X rays, *Plenum Press*, New York, USA (1986).

[17] D. Attwood, Soft x-ray and extreme ultraviolet radiation: principles and applications, *Cambridge University Press*, Cambridge, UK (1999).

[18] B. L. Henke, E. M. Gullikson and J. C. Davis, X-ray interactions: photoabsorption, scattering, transmission, and reflection at E=50-30000 eV, Z=1-92, At. Data Nucl. Data Tables 54 (2) (1993) 181-342.

[19] K. S. Chon, Y. Namba and K. H. Yoon, Optimization of a Wolter type I mirror for a soft X-ray microscope, *Prec. Eng*. 30 (2006) 223-230.

[20] J. Kirz, C. Jacobsen, and M. Howells, Soft x-ray microscopes and their biological applications, *Q. Rev*. *Biophys*. 28 (1) (1995) 33-130.

**Kwon Su Chon** received a PhD in Mechanical Engineering from Chubu University. He was a research professor at the Institute for Radiological Imaging Science. He has worked at the Department of Radiological Science in Catholic University of Daegu since 2009. His research is in the field of design and fabrication of X-ray optics and X-ray imaging system of nano and micro-spatial resolution.

**Yoshiharu Namba** graduated from the Department of Precision Engineering, Osaka University, in 1964, and received the Dr Eng degree from Osaka University in 1971. He was an associated professor at Osaka University from 1972 to 1987, and has been a professor at Chubu University since 1987. He was the winner of the David Richardson Medal from the Optical Society of America in 1998. He is a fellow of JSME and JSPE.